Crystal structure of human dehydroepiandrosterone sulphotransferase in complex with substrate

Peter H. REHSE, Ming ZHOU and Sheng-Xiang LIN[1]

Oncology and Molecular Endocrinology Research Center, Laval University Medical Center CHUL (CHUQ), 2705 Boul. Laurier, Quebec City, Quebec, G1V 4G2 Canada

Dehydroepiandrosterone sulphotransferase (DHEA-ST) is an enzyme that converts dehydroepiandrosterone (DHEA), and some other steroids, into their sulphonated forms. The enzyme catalyses the sulphonation of DHEA on the 3α-oxygen, with 3′-phosphoadenosine-5′-phosphosulphate contributing the sulphate. The structure of human DHEA-ST in complex with its preferred substrate DHEA has been solved here to 1.99 Å using molecular replacement with oestradiol sulphotransferase (37% sequence identity) as a model. Two alternative substrate-binding orientations have been identified. The primary, catalytic, orientation has the DHEA 3α-oxygen and the highly conserved catalytic histidine in nearly identical positions as are seen for the related oestradiol sulphotransferase. The substrate, however, shows rotations of up to 30°, and there is a corresponding rearrangement of the protein loops contributing to the active site. This may also reflect the low identity between the two enzymes. The second orientation penetrates further into the active site and can form a potential hydrogen bond with the desulphonated cofactor 3′,5′-phosphoadenosine (PAP). This second site contains more van der Waal interactions with hydrophobic residues than the catalytic site and may also reflect the substrate-inhibition site. The PAP position was obtained from the previously solved structure of DHEA-ST co-crystallized with PAP. This latter structure, due to the arrangement of loops within the active site and monomer interactions, cannot bind substrate. The results presented here describe details of substrate binding to DHEA-ST and the potential relationship to substrate inhibition.

Key words: alternate binding, DHEA, hydroxysteroid, steroid metabolism, substrate inhibition.

INTRODUCTION

In humans, dehydroepiandrosterone (DHEA) and its 3α-sulphonated form are the major circulating precursors to the sex hormones. These steroids are secreted in massive amounts by the adult human adrenal gland, with cholesterol being the only steroid that is found at higher levels in the blood. Although containing no intrinsic biological activity, these precursor steroids of adrenal origin account for the production of 30–50% of androgens in men and 75% of oestrogens in menstruating women. For postmenopausal women the contribution is 100% [1].

In target peripheral tissues, DHEA can be converted into sex hormones either directly or indirectly. The androgens testosterone and dehydrotestosterone, as well as the oestrogenic oestradiol, are formed from DHEA through the intermediate steroid androstenedione [2,3]. As with DHEA and 3α-sulphonated DHEA, the latter steroid has no intrinsic biological activity and is considered to be a sex hormone precursor. Which sex hormone is produced in the target tissues through androstenedione depends on the proportions of 17β-hydroxysteroid dehydrogenase (17β-HSD), 3β-HSD, 5α-reductase and aromatase activities present. In postmenopausal and young women, 80–100% of androst-5-ene-3β,17β-diol, another important oestrogen, is formed directly from DHEA by 17β-HSD.

The enzyme DHEA sulphotransferase (DHEA-ST; EC 2.8.2.2; subunit mass 34 kDa) catalyses the sulphonation of DHEA on the 3α-oxygen, with 3′-phosphoadenosine 5′-phosphosulphate (PAPS) contributing the sulphate. The sulphonated form of DHEA is not only more stable and hydrophilic, but it binds better to albumin and is the major circulating form of DHEA [4]. Dysfunction of DHEA-ST could lead to higher levels of DHEA in the plasma, which in turn could affect the production of the steroid hormones testosterone, dehydrotestosterone, oestradiol and androst-5-ene-3β,17β-diol. The abnormal regulation of these hormones could result in the formation of sex hormone-dependent tumours. For example, breast cancer is related to oestrogen production, while prostate cancer is related to androgen production. Both DHEA and its 3α-sulphonated form have been linked to cardiovascular disease [5], and reduced levels of DHEA-ST in the liver have been associated with chronic liver disease [6]. Although familial hyperandrogenicity in women is associated with high levels of DHEA due to non-classical 3β-HSD deficiency, there is no evidence of mutations in the genes encoding type 1 and type 2 3β-HSD [7,8], and therefore a potential candidate for the cause is defective DHEA-ST.

Another important area of research is the study of adverse side effects of drugs during therapy. Inhibition of human liver DHEA-ST activity by commonly prescribed drugs has been suggested as a novel mechanism of drug toxicity [8–10]. A study by Bamforth et al. [9] examined the effects of a large group of drugs on sulphotransferase activities in human liver cytosol preparations. Among these drugs, many exhibited side effects of sexual dysfunction and disruption of sex hormone action during clinical trials. It was found that clomiphene, testosterone, danazol and spironolactone were potent inhibitors of DHEA-ST, with IC_{50} values of $< 5\ \mu$M. Understanding substrate binding is a first step towards the improvement of existing drugs of a steroid nature.

Several forms of DHEA-ST have been characterized from different sources, such as the livers of rodents, guinea pig, bovine

Abbreviations used: DHEA, dehydroepiandrosterone; DHEA-ST, dehydroepiandrosterone sulphotransferase; EST, oestradiol sulphotransferase; HSD, hydroxysteroid dehydrogenase; PAP, 3′,5′-phosphoadenosine; PAPS, 3′-phosphoadenosine 5′-phosphosulphate.

[1] To whom correspondence should be addressed (e-mail sxlin@crchul.ulaval.ca).

and human, and the adrenal tissues of bovine and human [7,11–15]. The function and regulation of human DHEA-ST have been studied extensively [7,16–18], with the structure in complex with the desulphonated cofactor 3′,5′-phosphoadenosine (PAP) but in the absence of substrate having been solved by X-ray crystallography [19]. This latter enzyme is referred to here and in this previous paper [19] as SULT2A3, and differs in sequence from the structure described here as DHEA-ST by only a few residues at the C-terminus. The three-dimensional structure of a related enzyme, oestradiol sulphotransferase (EST), complexed with substrate and cofactor analogue has also been solved by X-ray diffraction [20]. However, in addition to having a different specificity, the sequence identity between these enzymes is quite low, at 37.6 %. Structural knowledge of DHEA-ST, especially in complex with substrate, will give us an opportunity to study in detail the mechanism of this important regulatory enzyme for sex hormones. A comparison with EST would broaden our understanding of steroid sulphotransferases, which, due to their effect in decreasing steroid hydrophobicity, have further relevance with respect to steroid detoxification [21]. The structure and function of sulphotransferases has been reviewed recently [22].

Human DHEA-ST has been expressed, purified and crystallized in our laboratory [10,23]. Here we report the crystallographic structure of the enzyme in complex with its preferred substrate, DHEA.

EXPERIMENTAL

Preparation and crystallization

Human DHEA-ST was purified in our laboratory. Briefly, recombinant human DHEA-ST, expressed as a glutathione S-transferase fusion protein in *Escherichia coli*, was purified using glutathione–Sepharose 4B affinity chromatography, followed by a Factor Xa cleavage step and Q-Sepharose Fast Flow column chromatography [23]. The conditions of crystal growth were also described previously [24]. DHEA-ST was co-crystallized with DHEA using a hanging-drop method by vapour diffusion at room temperature. The reservoir contained 100 mM Tris, pH 7.5, 1.2 mM $CoCl_2$ and 170 mM $(NH_4)_2SO_4$. Protein stocks contained 12 mg/ml (0.35 mM) DHEA-ST and 0.5 mM DHEA in 10 mM Tris, pH 7.5, 0.5 mM EDTA and 0.1 % n-octyl β-D-glucopyranoside. The hanging drop was initiated by mixing 1.8 μl of protein with 2.7 μl of reservoir solution. The crystals appeared after 2–3 days, and matured in 7–10 days.

Derivative preparation, flash-freezing, and data collection and processing

A 1.5 μl aliquot of 80 % glycerol was added into the drop before the thick plate-shaped crystals were passed through mineral oil and flash-frozen on the beam line. Data were collected at the X8C beam line at the National Synchrotron Light Source, Brookhaven National Laboratory, Upton, NY, U.S.A., using a Quantum-IV CCD imaging-plate detector. All data were processed using the HKL package [25]. The native data set was collected from a single flash-frozen crystal mounted 160 mm from the detector and rotated through 94° in increments of 1.0° (based on an estimated mosaicity of 0.4°). Data were processed to 2.15 Å with an R_{sym} of 4.9 % and completeness of 92.9 %. The completeness in the last resolution shell is 94.9 %. A total of 82583 measured observations was reduced to 22121 unique reflections. The crystal was primitive orthorhombic, with cell dimensions of $a = 74.46$, $b = 127.49$ and $c = 44.59$ Å, with a space group, based on systematic absences, of $P2_12_12$.

The $2KI \cdot HgI_2$ (Alpha) derivative was prepared by soaking a single crystal in 3 mM of heavy-atom solution for 3.5 h and then flash-freezing after a short back soak. The crystal was mounted 140 mm from the detector and rotated through 90° in increments of 1.5° due to an initial estimated mosaicity of 0.7°. Data were processed to 1.99 Å with an R_{sym} of 5.6 % and completeness of 93.1 %. The completeness in the last resolution shell is 93.5 %. A total of 116140 measured observations was reduced to 32429 unique reflections. The mercury derivative was non-isomorphic to the native enzyme, with cell dimensions of $a = 77.90$, $b = 137.96$ and $c = 45.87$ Å. Table 1 summarizes the data collection.

Structure determination and refinement

Structure solution was initially performed by molecular replacement using EST [20] as a model and the CNS software package [26]. A weak molecular replacement solution coupled with only 37 % identity with the model enzyme required caution in interpretation, and therefore a search for heavy-atom derivatives was instigated. The data set obtained through a $2KI \cdot HgI_2$ soak of the substrate-complexed crystal did give a clear molecular replacement solution, with the largest peak (0.243) 3 sigma units larger than the second largest peak (0.152). This solution corresponded to the strongest cross-rotation peak (0.0515), which was 1.2 sigma units larger then the second largest peak (0.0389). This peak, once origin shifts and cell dimension differences were taken into account, corresponded to the peak obtained with the native data. The $2KI \cdot HgI_2$ data set was non-isomorphous to

Table 1 Data processing statistics

Values in parentheses refer to the highest-resolution shell. $R_{sym} = \sum | I - \langle I \rangle | / \sum I$, where I is intensity (of a diffraction index).

Parameter	Native	$2KI \cdot HgI_2$ derivative
Number of images	94	60
Oscillation range (°)	1.0	1.5
Space group	$P2_12_12$	$P2_12_12$
Unit cells (Å)	$a = 74.46$, $b = 127.49$, $c = 44.59$	$a = 77.90$, $b = 137.96$, $c = 45.87$
Mosaicity (°)	0.44	0.51
Resolution range (Å)	20–2.15	40–1.99
Number of observations	82583	116140
Number of unique reflections	22121	32429
Redundancy	3.7	3.6
R_{sym} (%)	4.9 (29.5)	5.6 (55.5)
Completeness (%)	92.9 (94.9)	93.1 (93.5)
$\langle I/\sigma(I) \rangle$	19.4 (3.3)	17.6 (3.1)

the native data set. Self-rotation functions and a search for a second translation peak did not yield a second solution for either data set.

Refinement and solvent flattening was carried out using the CNS software package [26]; model rebuilding was carried out using program O [27]. The initial model was built into a solvent-flattened map derived from the molecular replacement. Composite omit maps were used throughout the model building to check for errors. The initial refinement cycles were performed using simulated annealing with torsion restraints, with starting temperatures of 5000 K, 2000 K and 1000 K. Each of the refinement cycles included both positional (200 cycles) and B-factor (50 cycles) refinement. Final positional and B-factor refinement weights were determined using CNS scripts. All refinement was performed using all data, with 10% removed randomly for calculation of R_{free}, maximum likelihood targets and bulk solvent corrections. After a few cycles of rebuilding and refinement, the correctness of the molecular replacement was further supported by strong bi-lobal density near Cys-55, Cys-154 and Cys-199. These three free cystines had formed bonds to the HgI_2 molecules. The positions of the HgI_2 corresponded to peaks from the anomalous Patterson maps. Rebuilding was switched to the native (non-derivative) data set using the model partially rebuilt from the derivative data set, but this was discontinued due to a persistently disordered loop near the active site. The structure of DHEA-ST, without substrate, in complex with desulphonated cofactor has been as published as SULT2A3, hydroxysteroid sulphotransferase [19]. This occurred during the rebuilding of DHEA-ST in our laboratory. However, in addition to a lower resolution (2.4 Å) and a different space group ($P2_12_12_1$; $a = 72.9$, $b = 97.2$ and $c = 128.4$ Å), substrate is excluded by loop conformations that penetrate the active site. The molecular replacement solution was confirmed using the cofactor-complexed DHEA-ST structure as model, and rebuilding continued.

The substrate-complexed crystal has now been rebuilt and refined to an R-factor of 23.1% with a free-R of 26.2% with CNS software. Residues 2–285 of the protein have been built into density, with the exception of the side chains beyond Cβ of Lys-248. A nine-residue linker to the fusion protein replaced residue 1. The density of this region is not well defined and its connection to residue 2 is unclear. There are no residues in disallowed regions of the Ramachandran plot. DHEA has been placed in density at the active site at two alternative conformations, with three HgI_2 molecules having been added, 216 water molecules and one iodine. The overlapping nature of the DHEA conformations became apparent after the structure was rebuilt and refined for several cycles. Although the HgI_2 molecules were easily placed in the early stages, the DHEA molecules were only added to the structure using F_o–F_c maps (where F_o and F_c are the observed and calculated structure factors respectively) during the final rounds of refinement. Based on a comparison of B-factors between the two DHEA molecules and the surrounding protein residues, an estimated occupancy of 50% for each substrate conformation was chosen.

The entire molecule, including substrate and water, was confirmed using composite omit maps and checked using PROCHECK [28]. Refinement information is summarized in Table 2.

Structural comparisons

Structural comparison studies using the DHEA-ST–substrate complex, the DHEA-ST–PAP [20] complex and EST [19] were performed using the lsq_ routines of program O [26]. The structure has been submitted to the Protein Data Bank as 1J99.

Table 2 Refinement statistics

$R_{cryst} = \sum || F_o | - | F_c || / \sum | F_o |$ (F_o and F_c are the observed and calculated structure factors respectively). R_{free} was calculated from 10% of the data. Active site refers to protein residues shown in Figure 4.

Parameter	Value
Number of atoms (non-hydrogen)	
Protein	2377
Substrate	42
Hg	3
I	7
Water	216
Solvent content (%)	66
R_{cryst} (%)	23.1
R_{free} (%)	26.2
Mean B factors (Å^2)	
Protein	40.23
Substrate	51.62
Active site	56.05
Water	50.57
All	41.37
Root mean square deviations	
Bond lengths (Å)	0.023
Bond angles (°)	2.1
Dihedral angles (°)	22.7
Improper angles (°)	1.13
Ramachandran plot statistics (%)	
In the most favoured regions	88.3
In additional allowed regions	11.7
In generously allowed regions	0.0
In disallowed regions	0.0

RESULTS AND DISCUSSION

The structure of DHEA-ST is an α/β fold with a central four-stranded β-sheet (Figure 1). Although the overall fold of EST and DHEA-ST is similar, there is quite a large amount of displacement of secondary structure and loops, resulting in a root mean square deviation of 0.56 Å between the two structures

Figure 1 Secondary structure of DHEA-ST showing DHEA and His-99 as a CPK (Corey–Pauling–Koltun) representation

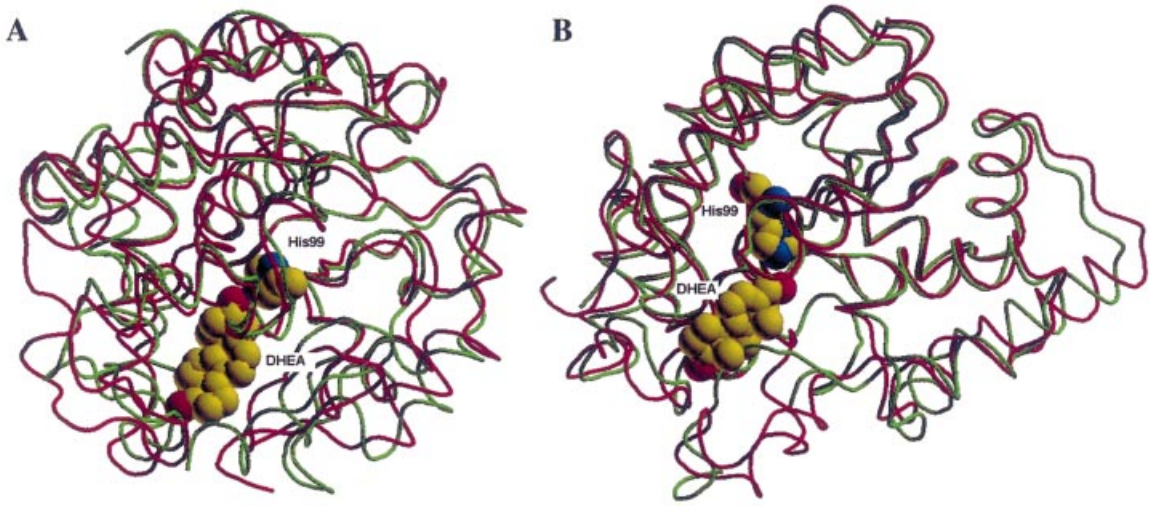

Figure 2 Wire representations of the overlapped main-chain atoms of sulphotransferases

DHEA and His-99 have been included as a CPK representation. The orientation of the molecule is chosen to highlight the loop variations around the substrate-binding site. Left panel: EST (green) and our DHEA-ST (red); right panel: SULT2A3 (green) and our DHEA-ST (red).

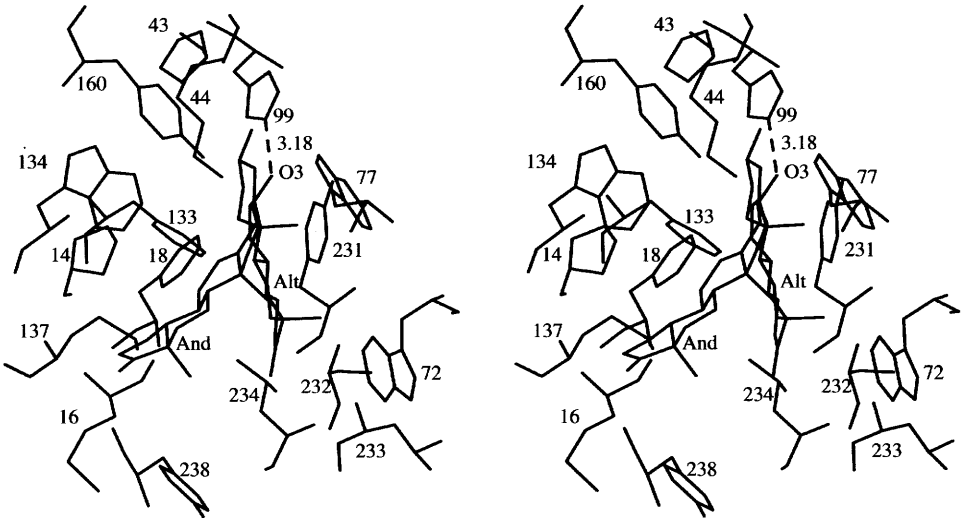

Figure 3 Substrate-binding site showing both the catalytic orientation (And) and the alternative orientation (Alt) that may be related to substrate inhibition

The hydrogen bond of O-3 of DHEA to Nε-2 of His-99 in the catalytic orientation is marked by a broken line, with the distance given in Å.

(Figure 2, left panel). For instance, in EST there is a five-stranded β-sheet, but the extra strand is displaced in the DHEA-ST structure. There is also a loss of two short stretches of β-sheet, due primarily to the deletion of several residues (see below). DHEA-ST and EST are classed as members of different sub-families of sulphotransferases [20]. When comparing the EST and DHEA-ST structures, the nucleotide-binding region contains more conserved residues than the substrate-binding region. This is reasonable, since they use the same cofactor but have different steroid specificities.

Catalytic substrate-binding site

As mentioned above, the structure of hydroxysteroid sulphotransferase has been solved in complex with the desulphonated cofactor PAP (SULT2A3) [19]. Although these crystals were grown under saturating concentrations of substrate, no electron density attributable to DHEA could be found at the active site. Using the EST structure to model the placement of the substrate, Pedersen et al. [19] indicated that the loop from Tyr-231 to Glu-244 would have to move to allow the substrate to bind, in addition to side-chain displacements of Trp-77 and Phe-133. Moreover, the second subunit of the biological dimer contributes to the locking in the substrate-blocking loop. It is clear that something has to give for substrate binding to occur. This could be loops, side chains or the dimer structure itself. These changes could also be accompanied by an altered substrate orientation.

The structure described below was from crystals obtained in the presence of saturated DHEA, but in the absence of PAP. It crystallized in a different space group from the SULT2A3

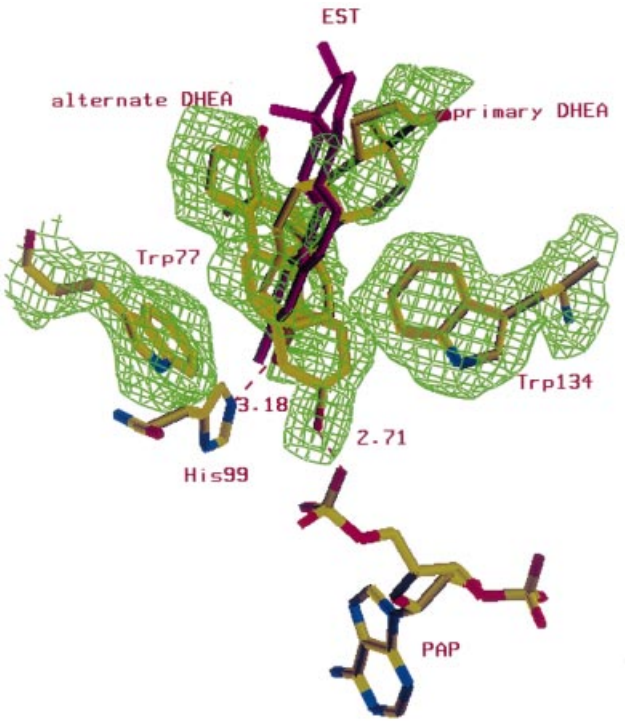

Figure 4 The two conformations of the DHEA substrate showing their relationship to His-99 and the modelled PAP

Trp-77 and Trp-134 have been added for perspective. The hydrogen bond from O-3 of DHEA in the catalytic orientation to Nϵ-2 of His-99 is marked by a dashed line, as is the distance between O-3 in the alternative DHEA orientation and the PAP phosphate group. Oestradiol modelled from the EST structure is shown in magenta. Electron density is a $2F_o–F_c$ simulated annealed map contoured at 1 sigma, with the DHEA molecules excluded from the calculations (F_o and F_c are the observed and calculated structure factors respectively). The distance is given in Å.

structure, with subunit interactions dissimilar to the stable dimer described by Pedersen et al. [19] (see below). Consequently, in our structure, the loop from Tyr-231 to Glu-244 is not constrained and, more importantly, electron density corresponding to the substrate is visible in DHEA-ST. This structure will be compared with both the substrate-bound EST structure and the non-substrate-containing SULT2A3 structure.

The structure described below has two substrate orientations within the active site (Figures 3 and 4). The catalytic orientation is identified through the position of O-3 of DHEA, which undergoes sulphonation. There is very little displacement of this atom between the EST and DHEA-ST structures (less than 0.5 Å), and even less between His-99 of DHEA-ST and His-108 of the EST, both of which form a hydrogen bond to the steroid O-3 through Nϵ-2. This histidine is strongly conserved among several sulphotransferases, including EST, phenol sulphotransferase, hydroxysteroid sulphotransferase and flavanol 3-sulphotransferase, suggesting a catalytic role [20]. Similarities end at this point; a comparison of the oestradiol in the EST structure and the DHEA in the DHEA-ST structure show that the two substrates are displaced quite dramatically, with rotations along the steroid plane (approx. 60°) and smaller rotations (approx. 10°) around the other two axes, coupled with a large number of substitutions and loop displacements surrounding the active site. In the case of DHEA-ST, a second (very weak) hydrogen bond to O-3 is formed with Nϵ-2 of Trp-77 (3.6 Å) that substitutes for Phe-81 of EST, which cannot fulfil the same function. The side-chain orientation of Phe-81 of EST is the same as the side-chain orientation of Trp-77 in the non-substrate-containing DHEA-ST. In both cases the aromatic side chain interacts with the substrate, but, as stated above, the substrate orientation differs. The second hydrogen bond in the EST structure is provided by Nϵ of Lys-106, which is substituted by Ser-97 in DHEA-ST.

In the DHEA-ST structure, O-17 of DHEA has one very weak hydrogen bond to the carbonyl oxygen of residue Tyr-238 (3.4 Å). Similar binding of O-17 to that seen with EST would be impossible, due to loop displacements. O-17 in the EST structure has a single weak hydrogen bond (3.0 Å) to the side chain of Asn-86; the most closely corresponding residue in the DHEA-ST structure is Met-16, whose side chain cannot form a hydrogen bond. Although the hydrogen bonding is weak, it is clear that the orientation of DHEA at the O-17 end is governed by the orientation of the surrounding loop structures.

In both DHEA-ST and EST there are a large number of hydrophobic residues surrounding the active site (within 6 Å). With the DHEA complex, several hydrophobic residues are in proximity to the substrate. These include the previously mentioned His-99 and Trp-77, as well as Phe-18, Tyr-231, Leu-234 and Met-137. However, only the side chains of the latter two are in direct van der Waal contact with the substrate. Taking the closest residues from the EST structure, we find that aromatic residues remain aromatic and aliphatic residues remain aliphatic. In addition, the side chains of residues Phe-160, Trp-72, Pro-14, Pro-43, Phe-133, Tyr-238, Trp-134 and Met-16 contribute to the hydrophobic nature of the active site. The last two residues have no corresponding contribution in the EST structure. Phe-133, which is considered to be highly conserved among sulphotransferases, is further away from the substrate than the corresponding arrangement in the EST structure. The main source of displacement appears to be insertion of the Tyr-134 side chain.

Of interest is a paired loop substitution near the active site. In the DHEA-ST structure the loop comprising residues 13–20, in addition to providing some hydrophobic stabilization, partially blocks access to the active site. This eight-residue loop is truncated by two residues in the EST structure, with a corresponding change in conformation, so that there is a difference of 5.9 Å between the furthest Cα extensions of the loops. The loss of the hydrophobic contribution from Pro-14 is compensated by a Phe-149 in the EST structure. Correspondingly, the loop comprising residues 79–84 gains five residues and two short β-sheets in the EST structure, resulting in an extension of 6.9 Å. The end result is that the extended versions of both loops have two Cα atoms within 2 Å of each other (see bottom of Figure 2, left panel).

A third, highly flexible region (residues 230–253) contributes to substrate binding. Parts of this loop diverge dramatically from the EST structure, and the loop contributes Tyr-238, Tyr-231 and Leu-234 to the hydrophobic environment of the active site. In the native (non-derivative) $P2_12_12$ structure this loop was so disordered that it could not be built properly, and it was for this reason that the $2KI \cdot HgI_2$ data set was used as the final data set for rebuilding. In the SULT2A3 structure this region also differs dramatically from our DHEA-ST structure (see bottom of Figure 2, right panel). In the SULT2A3 structure this loop prevents substrate binding and is involved in the dimer interface, suggesting that the dimer is an inactive form [19]. However, in our DHEA-complexed structure this dimer interaction does not exist. In the protein data bank submission for the SULT2A3 structure, the authors suggest that the dimer may not be the actual biological dimer, a postulate supported further by mutation studies [29]. It was shown by Chang et al. [23] that DHEA-

ST is a homodimer consisting of two identical subunits by gel filtration under various combinations of substrate and cofactor (H.-J. Chang and S.-X. Lin, unpublished work), yet none of the possible dimers in the various space groups show strong interactions. Comparing DHEA structures crystallized in the $P2_12_12_1$, $P222_1$ and $C222_1$ space groups (apo-enzyme), there does not appear to be any common dimer arrangement that can be considered to be the biological dimer [24]. When compared with the SULT2A3 structure, the loop displacement affects the position, but not so much the conformation, all the way back to residue 203. The divergence of the loop is not just a simple movement out of the substrate-binding site, but includes a reorientation of residues contributing to substrate stabilization, thereby indicating its important role in substrate binding. For example, Tyr-231 contributes to the stabilization of both the catalytic substrate orientation and the alternative substrate orientation described below. However, in the non-substrate-bound state, the aromatic group is rotated and moved away from the binding pocket, and is involved in the dimer interaction. The dual role of this loop appears to be central to the function of this enzyme.

With the exception of the above loop and some additional divergent regions (133–146 and 277–285), the overall structure of SULT2A3 differs little from our DHEA-ST structure. There is some sequence divergence due to the construction of a histidine tag for the SULT2A3 structure at the C-terminus. Cβ of residue Phe-139 moves 3.2 Å, primarily due to the dimer interaction of the SULT2A3 structure, where there is hydrophobic stacking to Tyr-238 and van der Waal conflict with Ala-91, although substrate may have some effect. There is some interaction of Phe-139 with a symmetry-related subunit around the C-terminus. A similar shift occurs for the side chains of Phe-133 and Trp-134, both of which are orientated perpendicular to the substrate. However, in this case the shift does not appear to be significant with respect to their binding contribution.

Alternative substrate-binding site

A second, 'alternative' substrate orientation exists, in addition to the catalytic orientation described above. In this binding mode the O-3 of DHEA is shifted 2.87 Å towards the non-sulphonated cofactor analogue (PAP) in comparison with the catalytic orientation. O-3 in the alternative orientation is within hydrogen-bonding distance of the modelled PAP phosphate (P-1) oxygen (2.71 Å), while of the catalytic orientation O-3 is 5.0 Å from this atom, allowing plenty of room for the sulphate of PAPS to be modelled in. PAP was modelled using the SULT2A3 structure [19]. Additionally, there is a 45° rotation of the steroid out of the steroid plane with respect to the catalytic orientation. The observation that O-3 in the alternative conformation is within hydrogen-bonding distance of the modelled PAP phosphate group suggests the possibility of a stable interaction between the desulphonated cofactor and substrate, which may prove to be the source of substrate inhibition observed for DHEA-ST [30,31] (Figure 4). His-99 does not form a hydrogen bond with O-3 in the alternative conformation. Nϵ of Lys-44, which has been suggested to have a catalytic role, does not form a hydrogen bond with DHEA in either substrate orientation; however, its amide nitrogen forms a hydrogen bond (3.3 Å) with O-3 in the alternative orientation. Substrate binding for either orientation requires the rotation of the side chain of Trp-77 from the position observed with the SULT2A3 structure. The orientation of this residue is stacked against the steroid in the alternative steroid orientation. Unlike in the catalytic orientation, where they are only in proximity, Phe-139, His-99, Trp-77, Tyr-231 and Trp-72 provide direct hydrophobic contacts with the substrate. The latter residue has also rotated from its position in the non-substrate-bound SULT2A3 structure to maximize the hydrophobic contact with the alternative substrate conformation.

Cofactor-binding site

As mentioned above, the PAP-binding sites of the EST and hydroxysteroid sulphotransferase structures share more conserved residues than the substrate-binding sites. In fact, there is good overlap between the EST and SULT2A3 structures. Both of these structures contain PAP, while our DHEA-ST does not. There are some changes that can be attributed directly to the absence of PAP, but others that could also be attributed to substrate binding. Most notable of the latter cases is Tyr-231, whose dual interaction with the substrate and dimerization has already been described. This residue also provides a hydrophobic interaction, with the PAP molecule (modelled in using the SULT2A3 structure) taking the place of Leu-245 in the SULT2A3 structure and Phe-255 in the EST structure. The hydroxy group could potentially form a hydrogen bond with the modelled PAP phosphate group. The side chain of Asn-48 forms a hydrogen bond with the PAP adenosine, but in the DHEA-ST structure (no PAP) it rotates to form a hydrogen bond with the hydroxy group of Tyr-231. The role of Tyr-231 in a ternary complex is worth examining further. The adenosine ring of PAP is partially responsible for the displacement of Tyr-220 and Met-223; however, in both cases the movement is further than van der Waal interactions would require. As mentioned above, the large movement of the loop comprising residues 230–255 affects the structure back to residue 203. A small movement of Ser-251 would be required to accommodate the PAP molecule. This residue is nowhere near the PAP molecule in the SULT2A3 structure; conversely, residues 245–249, which interact with the PAP molecule in the SULT2A3 structure, are orientated away from the cofactor-binding site in our substrate-containing structure. It does not appear that this loop is as crucial to PAP binding as it is to substrate binding, although it does play a part.

The exact relationship between cofactor and substrate binding remains unclear. As described in our crystallization paper [24], DHEA-ST was co-crystallized in the presence of the desulphonated cofactor PAP and DHEA. However, the space group was very similar to that reported by Pedersen et al. [19], where the enzyme was co-crystallized with PAP alone. Preliminary maps showed the same, DHEA-excluding, arrangement at the active site. Soaking the DHEA co-crystallized crystals reported in the present study in solutions containing PAP resulted in disrupted crystals. Clearly the presence of PAP has a major effect on the conformation of DHEA-ST. The search for a ternary complex continues in our laboratory.

We thank Dr Van Luu-The for providing the overproduction strain of DHEA-ST. This work was supported by the Canadian Space Agency and the Canadian Institute of Health Research.

REFERENCES

1 Labrie, F. (1991) Intracrinology. Mol. Cell. Endocrinol. **78**, C113–C118
2 Adams, J. B. (1985) Control of secretion and the function of C19-delta 5-steroids of the human adrenal gland. Mol. Cell. Endocrinol. **41**, 1–17
3 Labrie, F., Dupont, A. and Bélanger, A. (1985) Complete androgen blockade for the treatment of prostate cancer. In Important Advances in Oncology (de Vita, V. T., Hellman, S. and Rosenberg, S. A., eds.), pp. 193–217, J. B. Lippincott, Philadelphia, PA
4 Longcope, C. (1996) Dehydroepiandrosterone metabolism. J. Endocrinol. **150**, S125–S127
5 Khaw, K.-T. (1996) Dehydroepiandrosterone, dehydroepiandrosterone sulphate and cardiovascular disease. J. Endocrinol. **150**, S149–S153

6 Elekima, O. T., Mills, C. O., Ahmad, A., Skinner, G. R., Ramsden, D. B., Bown, J., Young, T. W. and Elias, E. (2000) Reduced hepatic content of dehydroepiandrosterone sulphotransferase in chronic liver diseases. Liver **20**, 45–50

7 Luu-The, V., Bernier, F. and Dufort, I. (1996) Steroid sulfotransferases. J. Endocrinol. **150**, S87–S97

8 Zérah, M., Rhéaume, E., Mani, P., Schram, P., Simard, J., Labrie, F. and New, M. I. (1994) No evidence of mutations in the genes for type I and type II 3 beta-hydroxysteroid dehydrogenase (3 beta HSD) in nonclassical 3 beta HSD deficiency. J. Clin. Endocrinol. Metab. **79**, 1811–1817

9 Bamforth, K. L., Dalgliesh, K. and Coughtrie, M. W. (1992) Inhibition of human liver steroid sulfotransferase activities by drugs: a novel mechanism of drug toxicity? Eur. J. Pharmacol. **228**, 15–21

10 Luu-The, V., Dufort, I., Paquet, N., Reimnitz, G. and Labrie, F. (1995) Structural characterization and expression of the human dehydroepiandrosterone sulfotransferase gene. DNA Cell Biol. **14**, 511–518

11 Ogura, K., Kajita, J., Norihata, H., Watanabe, T., Ozawa, S., Nagata, K., Yamazoe, Y. and Kato, R. (1990) cDNA cloning of the hydroxysteroid sulfotransferase STa sharing a strong homology in amino acid sequence with the senescence marker protein SMP-2 in rat livers. Biochem. Biophys. Res. Commun. **166**, 1494–1500

12 Demyan, W. F., Song, C. S., Kim, D. S., Her, S., Gallwitz, W., Rao, T. R., Slomczynska, M., Chatterjee, B. and Roy, A. K. (1992) Estrogen sulfotransferase of the rat liver: complementary DNA cloning and age- and sex-specific regulation of messenger RNA. Mol. Endocrinol. **6**, 589–597

13 Oeda, T., Lee, Y. C., Driscoll, W., Chen, H.-C. and Strott, C. A. (1992) Molecular cloning and expression of a full-length complementary DNA encoding the guinea pig adrenocortical estrogen sulfotransferase. Mol. Endocrinol. **6**, 1216–1226

14 Driscoll, W. J., Martin, B. M., Chen, H.-C. and Strott, C. A. (1993) Isolation of two distinct 3-hydroxysteroid sulfotransferases from the guinea pig adrenal. Evidence for 3 alpha-hydroxy versus 3 beta-hydroxy stereospecificity. J. Biol. Chem. **268**, 23496–23503

15 Wilborn, T. W., Comer, K. A., Dooley, T. P., Reardon, I. M., Heinrikson, R. L. and Falany, C. N. (1993) Sequence analysis and expression of the cDNA for the phenol-sulfating form of human liver phenol sulfotransferase. Mol. Pharmacol. **43**, 70–77

16 Falany, C. N., Comer, K. A., Dooley, T. P. and Glatt, H. (1995) Human dehydroepiandrosterone sulfotransferase. Purification, molecular cloning, and characterization. Ann. N.Y. Acad. Sci. **774**, 59–72

17 Parker, Jr, C. R., Stankovic, A. K., Falany, C. N. and Grizzle, W. E. (1995) Effect of TGF-beta on dehydroepiandrosterone sulfotransferase in cultured human fetal adrenal cells. Ann. N.Y. Acad. Sci. **774**, 326–328

18 Parker, Jr, C. R., Stankovic, A. K., Faye-Petersen, O., Falany, C. N., Li, H. and Jian, M. (1998) Effects of ACTH and cytokines on dehydroepiandrosterone sulfotransferase messenger RNA in human adrenal cells. Endocr. Res. **24**, 669–673

19 Pedersen, L. C., Petrotchenko, E. V. and Negishi, M. (2000) Crystal structure of SULT2A3, human hydroxysteroid sulfotransferase. FEBS Lett. **475**, 61–64

20 Kakuta, Y., Pedersen, L. G., Carter, C. W., Negishi, M. and Pedersen, L. C. (1997) Crystal structure of estrogen sulphotransferase. Nat. Struct. Biol. **4**, 904–908

21 Jakoby, W. B., Sekura, R. D., Lyon, E. S., Marcus, C. J. and Wang, J. L. (1980) Sulfotransferases. In Enzymic Basic of Detoxification, vol. 2 (Jakoby, W. B., ed.), pp. 199–228, Academic Press, New York

22 Negishi, M., Pedersen, L. G., Petrotchenko, E., Shevtsov, S., Gorokhov, A., Kakuta, Y. and Pedersen, L. C. (2001) Structure and function of sulfotransferases. Arch. Biochem. Biophys. **390**, 149–157

23 Chang, H.-J., Zhou, M. and Lin, S.-X. (2001) Human dehydroepiandrosterone sulfotransferase: purification and characterization of a recombinant protein. J. Steroid Biochem. Mol. Biol. **77**, 159–165

24 Zhou, M., Rehse, P. H., Chang, H.-J., Luu-The, V. and Lin, S.-X. (2001) Crystallization and preliminary crystallographic results of apo and complex forms of human dehydroepiandrosterone sulfotransferase Acta Crystallogr. Sect. D Biol. Crystallogr. **57**, 1630–1633

25 Otwinowski, Z. and Minor, W. (1997) Processing of X-ray diffraction data collected in oscillation mode. Methods Enzymol. **276**, 307–326

26 Brünger, A. T., Adams, P. D., Clore, G. M., Delano, W. L., Gros, P., Grosse-Kunstleve, R. W., Jiang, J.-S., Kuszewski, J., Nilges, N., Pannu, N. S. et al. (1998) Crystallography & NMR system: A new software suite for macromolecular structure determination. Acta Crystallogr. Sect. D Biol. Crystallogr. **54**, 905–921

27 Jones, T. A., Zou, J. Y., Cowan, S. W. and Kjeldgaard, M. (1991) Improved methods for binding protein models in electron density maps and the location of errors in these models. Acta Crystallogr. Sect. A Fund. Crystallogr. **47**, 110–119

28 Laskowski, R. A., MacArthur, M. W., Moss, D. S. and Thornton, J. M. (1993) PROCHECK – A program to check the stereochemical quality of protein structures. J. Appl. Crystallogr. **26**, 283–291

29 Petrotchenko, E. V., Pedersen, L. C., Borchers, C. H., Tomer, K. B. and Negishi, M. (2001) The dimerization motif of cytosolic sulfotransferases. FEBS Lett. **490**, 39–43

30 Falany, C. N. (1997) Enzymology of human cytosolic sulfotransferases. FASEB J. **11**, 206–216

31 Otterness, D. M., Wieben, E. D., Wood, T. C., Watson, W. G., Madden, B. J., McCormick, D. J. and Weinshilboum, R. M. (1992) Human liver dehydroepiandrosterone sulfotransferase: molecular cloning and expression of cDNA. Mol. Pharmacol. **41**, 865–872

Received 21 September 2001/17 December 2001; accepted 12 February 2002